

# Uncertainty Quantification in Stereo Matching

Wenxiao Cai<sup>1,3</sup>, Dongting Hu<sup>2</sup>, Ruoyan Yin<sup>4</sup>, Jiankang Deng<sup>5</sup>, Huan Fu<sup>6</sup>, Wankou Yang<sup>1\*</sup>, Mingming Gong<sup>2</sup>

<sup>1</sup> Southeast University <sup>2</sup> The University of Melbourne <sup>3</sup> Stanford University

<sup>4</sup> National University of Singapore <sup>5</sup> Imperial College London <sup>6</sup> Alibaba Group

## Abstract

*Stereo matching plays a crucial role in various applications, where understanding uncertainty can enhance both safety and reliability. Despite this, the estimation and analysis of uncertainty in stereo matching have been largely overlooked. Previous works often provide limited interpretations of uncertainty and struggle to separate it effectively into data (aleatoric) and model (epistemic) components. This disentanglement is essential, as it allows for a clearer understanding of the underlying sources of error, enhancing both prediction confidence and decision-making processes. In this paper, we propose a new framework for stereo matching and its uncertainty quantification. We adopt Bayes risk as a measure of uncertainty and estimate data and model uncertainty separately. Experiments are conducted on four stereo benchmarks, and the results demonstrate that our method can estimate uncertainty accurately and efficiently. Furthermore, we apply our uncertainty method to improve prediction accuracy by selecting data points with small uncertainties, which reflects the accuracy of our estimated uncertainty. The codes are publicly available at <https://github.com/RussRobin/Uncertainty>.*

## 1. Introduction

Stereo matching, or binocular depth estimation, has long been a meaningful problem with numerous important applications in autonomous driving [14, 37], robot navigation [31, 42], industrial quality control [15] and medical image processing [33, 50]. Uncertainty estimation in depth estimation is crucial and has many real-world applications. In autonomous driving, for example, depth estimation accuracy should decrease in foggy days. If the car knows that uncertainty in estimation is large in such circumstance, it can make further decisions (e.g. slowing down to look more carefully) [35, 40]. Therefore, it is crucial to recognize uncertainties in stereo matching.

Uncertainty can be classified into two main cate-

gories: data uncertainty and model uncertainty [25]. Data (aleatoric) uncertainty arises from the inherent uncertainty in the data generation process, while model (epistemic) uncertainty stems from the inadequacy of the fitted model and the stochastic nature of model parameters, which can be reduced by increasing the amount of training observation [28]. Separately estimating these uncertainties provides several key advantages:

- Data uncertainty can help filter high-quality data: Points with high data uncertainty may result from errors in the data collection process and might not reflect the true ground truth. Identifying such points allows us to filter low-quality data, leading to a cleaner, more robust dataset that better supports accurate model training.
- Model uncertainty guides data collection: Separate estimates of model uncertainty can highlight data regions where the model is most uncertain, which often indicates a need for more training samples.

Estimating data and model uncertainty in stereo matching presents several challenges: (i) Existing frameworks [38, 48] primarily focus on estimating total uncertainty without disentangling it into its constituent sources, namely data and model uncertainty. (ii) Estimating data uncertainty requires knowledge of the disparity distribution, a task that remains unclear within current learning frameworks for stereo matching. (iii) Estimating model uncertainty often involves methods that necessitate multiple retrainings, such as deep ensembles [24, 34], leading to slower processing speeds and substantial computational demands.

We address these issues by (i) estimating Bayes risks of an ideally optimal model and current model as total and data uncertainty. Model uncertainty is measured by the excess risk between the current and optimal models. (ii) We introduce a framework that estimates the probability distribution of disparity values with ordinal regression [17]. Data uncertainty is derived from the variance within this distribution, (iii) while model uncertainty is obtained through an additional kernel-based estimator applied to model embeddings. This approach provides separate estimates for data and model uncertainty efficiently, without requiring model

\*Corresponding author: wkyang@seu.edu.cn

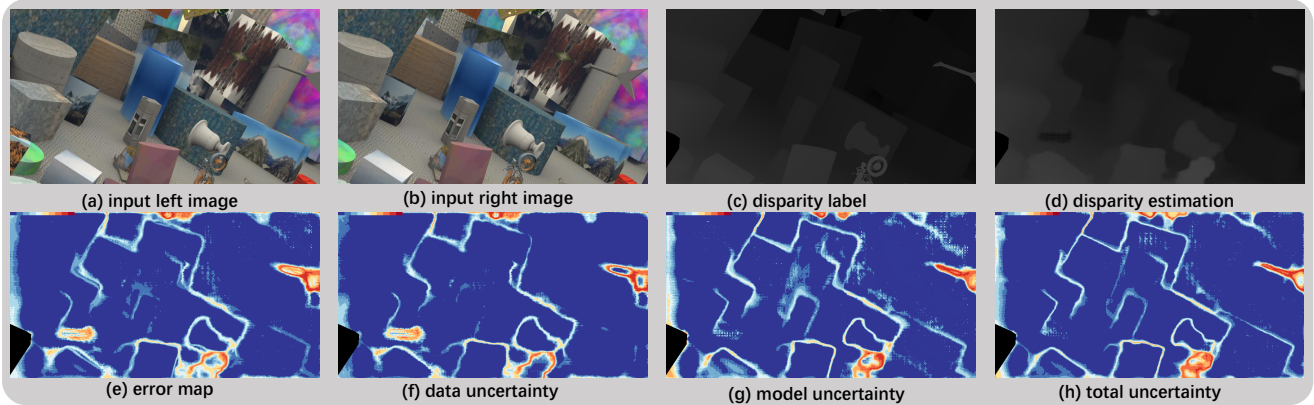


Figure 1. (a)(b): inputs of stereo matching. (c)(d): disparity ground truth and prediction. (e): disparity prediction error. (f)(g)(h): Our estimation of data, model and total uncertainty. The estimated uncertainty aligns well with prediction error.

retraining.

Experimental result on four widely used stereo matching datasets [18, 20, 39, 53] show that our proposed method has a more reliable estimation of data and model uncertainty. Moreover, we demonstrate that prediction accuracy can be improved by selecting data points with small uncertainties.

The contributions of our paper are:

- We leverage ordinal regression to make disparity predictions and calculate data uncertainty. The estimated uncertainty aligns well with disparity estimation error.
- We leverage parameters of an extra kernel regression model to save time in model uncertainty quantification.
- We illustrate the effectiveness of our estimated uncertainty in enhancing prediction accuracy by effectively filtering out highly uncertain data.

## 2. Related Work

In this section, we introduce recent works in stereo matching, depth estimation, and uncertainty estimation. The calculation and application of uncertainty in stereo matching is also explored.

**Uncertainty quantification.** Uncertainty is an important topic, and there are many efforts attempting to quantify and decouple data and model uncertainty. [28] proposed the use of a Bayesian deep learning framework for estimating uncertainty, considering both data and model uncertainty. Most methods utilize MC Dropout [7, 12, 19], Deep Ensemble [24, 34], and Variational Inference (VI) [4, 10, 11] to compute model uncertainty, resulting in prolonged computational time. Deep Evidential Regression [2] suggests that uncertainty arises from a higher-dimensional distribution, thereby avoiding the time and computational costs associated with repeated model training. NUQ [1, 30, 41], through a posterior approach, trains Kernel Density Estimation (KDE) or Gaussian Mixture Model (GMM) to estimate

model and data uncertainty.

### Stereo matching and binocular depth estimation.

Stereo matching, disparity estimation, and binocular depth estimation are similar concepts because disparity and depth can be converted into each other:  $disparity = f*B/\text{depth}$ , where  $f$  is the focal length, and  $B$  is the baseline distance between two cameras. Typically, features from left and right images are used to build cost volumes with cross-correlation or concatenation, followed by a 2D or 3D convolutional neural network [3, 5, 29, 44, 45, 47, 54]. GwcNet [21] is a state-of-the-art model which constructs the cost volume by group-wise correlation. We use GwcNet as the backbone for depth estimation.

**Uncertainty in depth estimation.** ELFNet [38] and UCFNet [48] employ non-deep-learning methods to calculate uncertainty in stereo depth estimation [9, 22], which is then utilized in downstream tasks such as transfer learning. SEDNet [6] incorporates an uncertainty module after the depth estimation network, employing KL divergence to have the uncertainty module learn the distribution of depth estimation errors as uncertainty. Deep distribution regression [36] was adopted in monocular depth estimation to estimate data uncertainty [23]. In this paper, we use ordinal distribution regression to learn the distribution of disparity and compute the data uncertainty by its variance. A time-saving but accurate method is adopted to estimate model uncertainty.

## 3. Proposed Method

We use Bayes risk for decomposition because it directly quantifies the model’s risk by measuring the discrepancy between predictions and ground truth. This decomposition is suitable for uncertainty quantification in stereo matching as it effectively captures uncertainties arising from data noise and model error in depth estimation. In this sec-

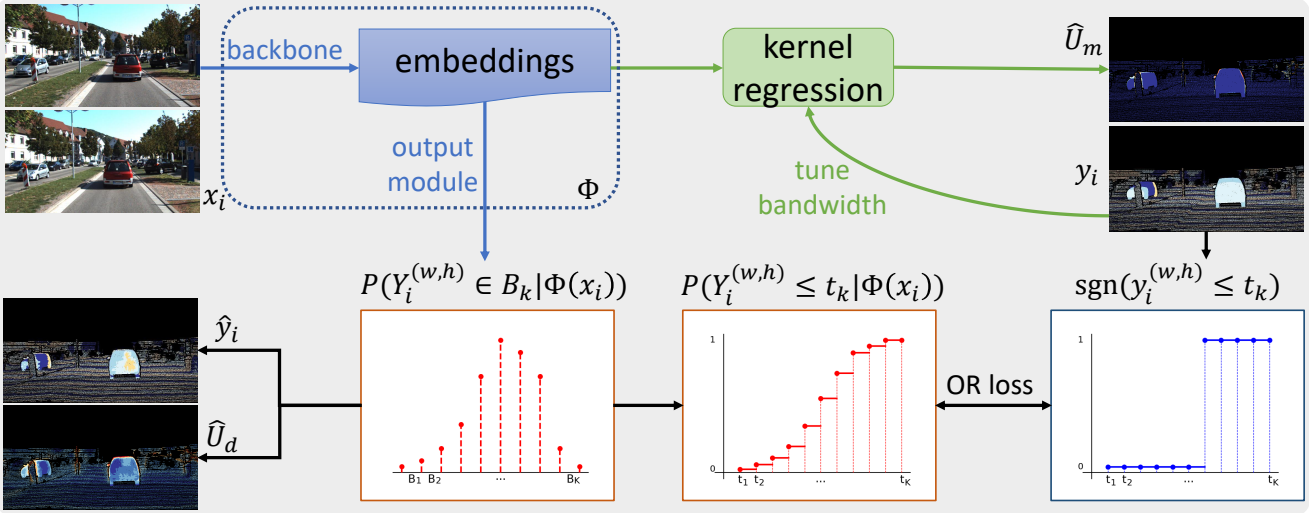


Figure 2. Pipeline of the proposed stereo matching and uncertainty quantification method. Ordinal regression model is adopted to estimate PMF of disparity. Prediction is the expectation of PMF, and data uncertainty is PMF’s variance. The model is supervised by the ordinal label, using ordinal regression loss. Model uncertainty is estimated with a kernel regression model, which is fitted on the embeddings of OR model.

tion, we first show the definition of uncertainty as Bayes risks [30]. Then we illustrate our data-driven uncertainty estimation method in stereo matching. We use Ordinal Regression (OR) [17] to estimate disparity (or depth) distribution. Model uncertainty is calculated from parameters of an extra Kernel Regression (KR), fitted on the embedding of OR model. The pipeline is shown in Fig. 2.

### 3.1. Definition of Uncertainty

Let two random variables  $X$  and  $Y$  denote the input stereo images and the disparity, respectively. Consider a training set  $D_{train} = \{x_i, y_i\}_{i=1}^N$  drawn from an unknown joint distribution  $D$ , the optimal rule  $g^*$  can be learned by minimizing the expected risk  $R(g) = E_{(X,Y) \sim D} l(g(X), Y)$ , where  $l$  is a loss function, and the rule  $\hat{g}$  trained on observations from  $D$  is the minimizer of the empirical risk  $R_N(g) = \frac{1}{N} \sum_{i=1}^N l(g(x_i), y_i)$ . For reader’s convinience of understanding, we first show total and data uncertainty ( $U_t, U_d$ ) definitions in classification problems:

$$U_t = P(\hat{g}(X) \neq Y | X = x), U_d = P(g^*(X) \neq Y | X = x). \quad (1)$$

Data uncertainty is the Bayes risk of the best model  $g^*$  fitted on the whole data distribution  $D$ . Total uncertainty measures the probability of error, of model  $\hat{g}$ . As model uncertainty reflects the imperfection of fitted model  $\hat{g}$  in comparasion to  $g^*$ , we can define it as:

$$U_m = U_t - U_d. \quad (2)$$

In the regression problem of stereo depth estimation, a

similar definition is used [30]:

$$\begin{aligned} U_t &= E [(\hat{g}(X) - Y)^2 | X = x], \\ U_d &= E [(g^*(X) - Y)^2 | X = x], \\ U_m &= U_t - U_d. \end{aligned} \quad (3)$$

Since  $g^*$  is fitted on whole distribution  $D$ , it should be:  $g^*(X) = E[Y|X]$ . As a result,  $U_d = E [(g^*(X) - Y)^2 | X = x] = \text{Var}[Y|X = x]$ . From this definition, it is evident that data uncertainty is an inherent characteristic of the data itself and is independent of the model or method used for estimation.

It is essential to note that while uncertainty and error are closely related, they are not the same concept. Error typically refers to the difference between the model’s prediction and the true value, whereas uncertainty focuses on error in the whole distribution  $D$ . For long-tail distribution or OOD data, a model have to chance to luckily exhibit a small error but it should always detect a high uncertainty.

### 3.2. Stereo Matching and Data Uncertainty Estimation

In data-driven uncertainty estimation, we estimate uncertainty  $U_d$  on observation dataset. Estimated data uncertainty  $\hat{U}_d$  is obtained by estimating distribution of  $Y$ :

$$U_d = \text{Var}[Y|X], \hat{U}_d = \text{Var}[\hat{Y}|X]. \quad (4)$$

We propose to use an ordinal regression (OR) model to estimate disparity distribution in stereo matching. Thus the estimation of disparity  $\hat{Y}_i$  and estimation of data uncertainty  $\hat{U}_d$  can be obtained by the mean and variance of estimated

distribution. For disparity within the range  $[\alpha, \beta]$ , we divide it into  $K$  bins.  $B_k = (t_{k-1}, t_k]$ , where:

$$t_k = \alpha + k(\beta - \alpha)/K, \text{ for } k \in \{0, 1, \dots, K\}. \quad (5)$$

OR tries to predict the probability of a pixel's disparity falling into  $B_k$ . For an image  $x_i$  of width  $W$ , height  $H$ , and channel  $C$ , and OR model  $\Phi$ , the feature map  $\eta_i = \Phi(x_i)$  is of size  $(W, H, K)$ . Here  $K$  is the features dimension, and also the number of bins. For a pixel at position  $(w, h)$ , the  $K$  values output by the softmax layer represent the probabilities of disparity  $Y_i^{(w,h)}$  falling into the  $K$ th bin, i.e., the conditional probability mass function (PMF):

$$P(Y_i^{(w,h)} \in B_k | \Phi(x_i)) = \frac{e^{\eta_{i,k}^{(w,h)}}}{\sum_{j=1}^K e^{\eta_{i,k}^{(w,h)}}}, \quad (6)$$

for  $k \in \{1, 2, \dots, K\}$ .

We recast the stereo matching problem to a series of binary classification tasks answers: what is the probability of the disparity value being less or equal to  $t_k$ ? To do so, we first convert the PMF to the conditional cumulative distribution function (CDF) by summing PMF values:

$$P(Y_i^{(w,h)} \leq t_k | \Phi(x_i)) = \sum_{j=1}^k P(Y_i^{(w,h)} \in B_k | \Phi(x_i)). \quad (7)$$

CDF is the likelihood of a pixel's disparity value less or equal to threshold  $t_k$ . To estimate the likelihood of a pixel's disparity less or equal to  $t_k$ , we adopt binary classification loss for each  $t_k$ , and sum them up as the OR loss. For ground truth disparity image  $y_i$ , loss  $l$  of a pixel and loss  $L$  for an image are expressed as:

$$\mathcal{P}_i^{(w,h)} = \log(P(Y_i^{(w,h)} \leq t_k | \Phi(x_i))), \quad (8)$$

$$l(x_i, y_i^{(w,h)}, \Phi) = - \sum_{k=1}^K \left[ \text{sgn}(y_i^{(w,h)} \leq t_k) \mathcal{P}_i^{(w,h)} + (1 - \text{sgn}(y_i^{(w,h)} \leq t_k)) (1 - \mathcal{P}_i^{(w,h)}) \right], \quad (9)$$

$$L(x_i, y_i, \Phi) = \frac{1}{WH} \sum_{w=0}^{W-1} \sum_{h=0}^{H-1} l(x_i, y_i^{(w,h)}). \quad (10)$$

The estimator  $\hat{\Phi} = \text{argmin}_{\Phi} \sum_{i=1}^N l(x_i, y_i, \Phi)$  is trained on dataset  $D_{train}$ , which consist of  $N$  pixels. We consider the expectation of conditional PMF as our disparity estimation  $\hat{y}^{(w,h)}$ . Since the variance of  $Y$  distribution is its data

uncertainty, we consider variance of estimated conditional PMF as estimated data uncertainty  $\hat{U}_d$ :

$$\hat{y}^{(w,h)} = \frac{1}{K} \sum_{k=1}^K \frac{t_k + t_{k+1}}{2} P(Y_i^{(w,h)} \in B_k | \Phi(x_i)), \quad (11)$$

$$\hat{U}_d^{(w,h)} = \sum_{k=1}^K \left( \frac{t_k + t_{k+1}}{2} - E \left[ \hat{y}^{(w,h)} | x; \hat{\Phi} \right] \right) P(Y_i^{(w,h)} \in B_k | \Phi(x_i)). \quad (12)$$

Intuitively, variance of distribution reflects the spread of predicted probability mass. If the variance is small, (e.g. 99% for one bin  $B_{11}$  and 1% for another one), the model is sure that the disparity value should fall in  $B_{11}$  and uncertainty should be small. If the variance is larger, (e.g. 33% for bin  $B_{10}$ ,  $B_{11}$  and  $B_{12}$ ), the model is unsure of which bin the disparity should fall into. Thus uncertainty should be larger. However, for each case, the expectation of distribution should be somewhere around  $B_{11}$ . So the predicted disparity should fall into  $B_{11}$  with different uncertainties.

In stereo matching, apart from estimating disparity, one may also estimate depth, since disparity and depth has one-to-one correspondence:  $\text{depth} = f * B / \text{disparity}$ , where  $f, B$  are focal length and baseline length of the camera pair. Due to the ordinal nature of depth, we suggest to use another binning method [17]:

$$t_k = \exp [\log(\alpha) + k \log(\beta/\alpha)/K], \text{ for } k \in \{0, 1, \dots, K\}. \quad (13)$$

### 3.3. Model Uncertainty Estimation

Model uncertainty is represented by the excess risk between total and data uncertainty.  $g^*$  is fitted on the whole distribution  $D$  and is optimal on  $D$ 's observation sets  $D_{train}$  and  $D_{test}$ .  $\hat{g}$  is fitted on  $D_{train}$ , as an approximation of  $g^*$ . According to Eq. 3, data uncertainty  $U_d$  corresponds to Bayes risk of  $g^*$ :  $U_d = E[(g^*(X) - Y)^2 | X = x]$ , and total uncertainty  $U_t$  corresponds to Bayes risk of  $\hat{g}$ :  $U_t = E[(\hat{g}(X) - Y)^2 | X = x]$ . The excess risk  $E[(\hat{g}(X) - Y)^2 | X = x] - E[(g^*(X) - Y)^2 | X = x]$  can be seen as the imperfectness of model  $\hat{g}$ . Thus it corresponds to model uncertainty  $U_m$ . Let's consider a particular estimator  $g$  first and then find the difference between  $g^*$  and  $\hat{g}$ .

We choose Kernel Regression (KR) model because it allows for a simple mathematical description of difference between  $g^*$  and  $\hat{g}$  [49]. We train KR model on the embeddings of the OR model  $\eta_i^{(w,h)}$  and corresponding disparity label:  $Y_i^{(w,h)}$  ( $i \in \{1, \dots, N\}, w \in \{1, \dots, W\}, h \in \{1, \dots, H\}$ ). To express it clearly, we denote the KR dataset in this section as  $\{s_i, t_i\}_{i=1}^M$  ( $M = H * W * N$ ). Let  $K_h$  denote the kernel function, kernel regression estimator  $\hat{g}$  is defined as:

Table 1. Disparity estimation and uncertainty quantification performance of GwcNet [21], SEDNet [6] and our proposed method. Uncertainty estimation performance is measured by AUSE. We also measure mean of data and model uncertainty. We mark the best result (except for full dataset results) in **bold** text.

Method	Dataset	EPE $\downarrow$	Uncert.	Mean of Uncert.		Dataset	EPE $\downarrow$	Uncert.	Mean of Uncert.	
			AUSE $\downarrow$	Data	Model				Data	Model
GwcNet+var		1.073	57.96	2.12	-		0.899	59.86	2.08	-
GwcNet+var+BS		1.073	45.07	2.12	4.48		0.899	52.11	2.08	4.20
GwcNet+E+BS		1.073	43.96	1.38	4.48		0.899	59.30	1.24	4.20
GwcNet+conf+BS		1.073	41.48	0.57	4.48		0.899	52.74	0.53	4.20
SEDNet(smooth-l1)		1.066	177.41	0.99	-		<b>0.698</b>	176.18	0.99	-
SEDNet(KG)	KITTI	1.070	48.45	0.90	-	VK2	0.910	157.33	0.89	-
SEDNet(UC)		1.021	29.07	0.36	-		0.890	163.71	0.82	-
SEDNet(UC)+TSUD		1.302	28.75	0.34	-		0.987	154.22	0.83	-
Ours		1.126	23.25	2.15	3.22		0.742	15.38	4.39	4.22
Ours+TSUD		<b>1.006</b>	<b>20.58</b>	2.08	3.11		<b>0.621</b>	<b>13.01</b>	4.30	4.14
Full dataset SEDNet		0.754	32.58	0.34	-		0.447	20.065	0.36	-
GwcNet+var		1.394	43.30	9.27	-		1.010	71.85	1.50	-
GwcNet+var+BS		1.394	32.62	9.27	9.41		1.010	63.11	1.50	2.51
GwcNet+E+BS		1.394	33.07	1.48	9.41		1.010	63.05	1.35	2.51
GwcNet+conf+BS		1.394	33.22	0.58	9.41		1.010	65.84	0.55	2.51
SEDNet(smooth-l1)		1.041	172.43	0.99	-		<b>0.789</b>	89.34	0.99	-
SEDNet(KG)	SF	1.225	36.84	1.17	-	DS	0.902	87.53	0.98	-
SEDNet(UC)		<b>1.033</b>	181.07	0.99	-		0.889	88.38	0.96	-
SEDNet(UC)+TSUD		1.099	170.22	0.99	-		0.846	85.05	0.95	-
Ours		1.145	<b>11.84</b>	12.73	10.22		0.810	41.29	2.42	2.36
Ours+TSUD		1.135	11.91	12.70	10.07		<b>0.725</b>	<b>38.20</b>	2.21	2.15
Full dataset SEDNet		0.567	191.84	0.99	-		0.578	70.75	0.99	-

$$\hat{g}(s) = \frac{\sum_{i=1}^M K_h(s - s_i) t_m}{\sum_{i=1}^M K_h(s - s_i)}. \quad (14)$$

According to [49], the difference between  $g^*$  and  $\hat{g}$  converges in a Gaussian distribution:

$$g^*(x) - \hat{g}(x) \rightarrow \frac{C}{N} \frac{\sigma^2(x)}{p(x)}, \quad (15)$$

where  $C$  is a constant related to kernel and bandwidth,  $N$  is the number of data in observation set,  $\sigma^2$  is the variance of  $x$  in the observation set, and  $p(x)$  is the marginal distribution of covariates. An asymptotic approximation of  $g^*(x) - \hat{g}(x)$  is used in estimating  $U_m$ :  $U_m = 2\sqrt{\frac{2}{\pi} \frac{C \sigma^2(x)}{N p(x)}}$  (details in [30]).

In kernel regression of our work, an RBF Kernel is adopted:

$$K_h(x, x_i) = \exp\left(-\frac{(s - s_i)^2}{2}\right), \quad (16)$$

where  $\sigma$  is the bandwidth, and  $K_h$  is the sum of all dimensions of  $s$ . K-Nearest Neighbours(KNN) is adopted in KR to further reduce computational costs. KR is a post-process fashion and does not require retraining the whole

OR model, making it faster compared to methods such as Deep Ensemble [24, 34] and Bootstrapping like Wild and Multiplier Bootstrap [8, 52].

## 4. Experiments

### 4.1. Datasets

We adopt 4 datasets in stereo matching: KITTI [20], Virtual KITTI [18], SceneFlow [39] and Driving Stereo [53]. As most of these datasets are relatively comprehensive, if all were used for training, the resulting data uncertainty would be much larger than model uncertainty. However, in real-world scenarios, the datasets used for training models are only a small portion. In other words, currently, we cannot train a universally applicable model; the model will always encounter situations in the real world that were not seen in the training set, i.e., situations with high model uncertainty. To simulate this situation in reality and to measure the ability of our method to estimate both data uncertainty and model uncertainty, we only use a small portion of the datasets for training or crosstraining of different versions of a dataset.

KITTI [20] has two versions, 2012 and 2015, each con-

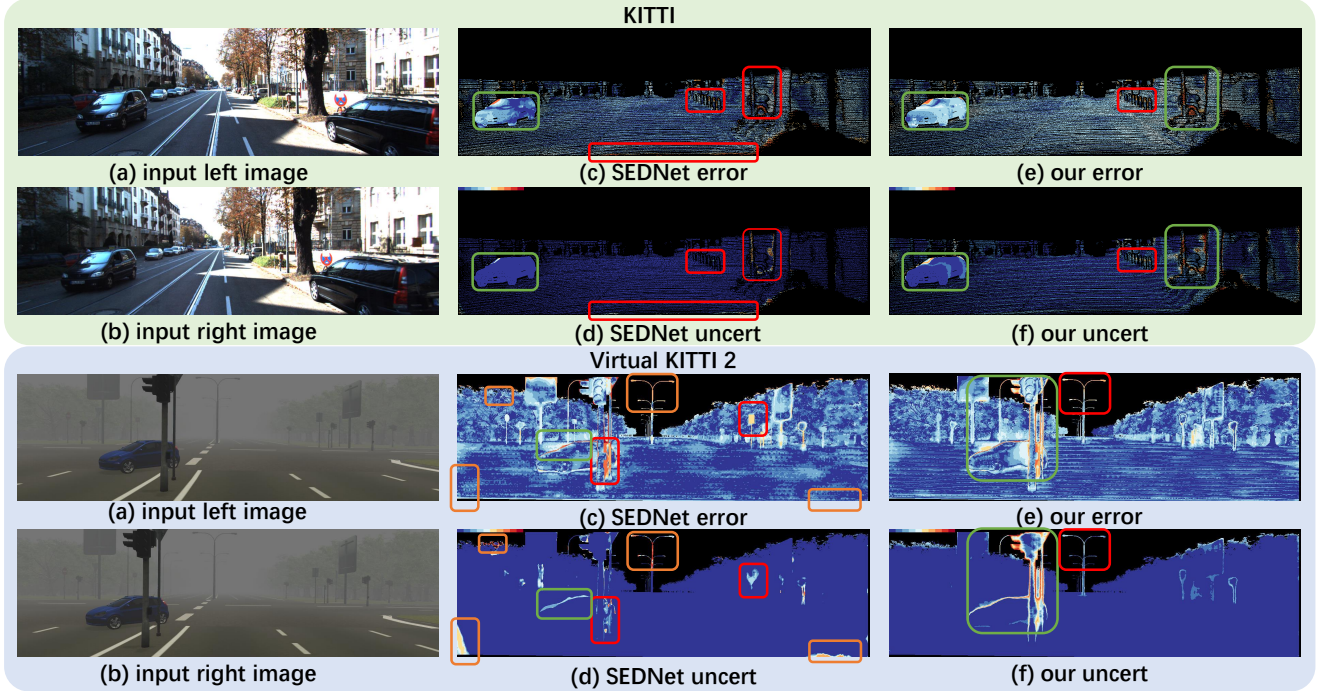


Figure 3. Experimental results of KITTI [20] and Virtual KITTI [18]. Red box: Large error, small uncertainty—model fails to predict large errors. Orange box: Small error, large uncertainty—model is overly cautious. Green box: uncertainty aligns well with error.

taining 180 training image pairs sized 1248x384. We use all images from KITTI 2015 and randomly select 10 images from KITTI 2012 for training, with model testing on KITTI 2012.

**Virtual KITTI** [18] is a synthetic dataset consisting of 21260 image pairs sized 1242x375. We randomly select 2000 pairs for training.

**SceneFlow** [39] images are sized 960x540 and consist of 35454 training and 4370 test stereo pairs. We use the final-pass version and randomly select 2000 images for training.

**DrivingStereo** [53] contains 174437 training and 7751 test stereo pairs, sized 881x400. We randomly select 2000 pairs for training.

We ensured that the model’s ability to predict disparity reached a baseline performance. To validate this, we compared the accuracy of disparity estimation of the model trained on the entire dataset, denoted as Full dataset SEDNet in Table 1, with the results obtained from training on subsets.

## 4.2. Metrics, Baselines and Results

**Metrics.** Our metrics consist of two parts: the model’s ability to estimate disparity and its ability to estimate uncertainty. Endpoint error (EPE) [13, 26] is used to measure the difference between the model’s estimated disparity and the ground truth. Area Under the Sparsification Error (AUSE) [27] between disparity and EPE is used to measure

the quality of uncertainty estimation: pixels are sorted by EPE from smallest to largest, and each time 1% of the pixels with the largest EPE are removed to calculate the Area Under Curve (AUC<sub>gt</sub>). Similarly, pixels are sorted by uncertainty from smallest to largest, and AUC<sub>est</sub> is calculated. AUC<sub>est</sub> – AUC<sub>gt</sub> yields AUSE, with smaller values indicating better uncertainty estimation. AUSE is normalized over EPE to eliminate the factor of prediction accuracy.

**Baselines.** On softmax output layer of GwcNet [21], we calculate its variance (GwcNet+var), entropy (GwcNet+E) and negative confidence (GwcNet+conf) as data uncertainty. We adopt bootstrapping [52] (BS) on GwcNet as model uncertainty. To calculate total uncertainty, according to definition of uncertainty 3, we directly sum up data and model uncertainty. SEDNet [6] with GwcNet backbone is compared, training with smooth-l1 [21], log-likelihood [28](KG) and divergence [6](UC) loss.

## 4.3. Results

Due to the use of ordinal regression loss, our approach pays more attention to the distribution of disparity, while methods such as GwcNet [21] and SEDNet [6] utilize L1 loss to directly supervise the values of disparity. As a result, our method performs slightly worse in terms of disparity estimation, with higher EPE. Please refer to Table. 1 for results. Qualitative results are shown in Fig. 3, 4.

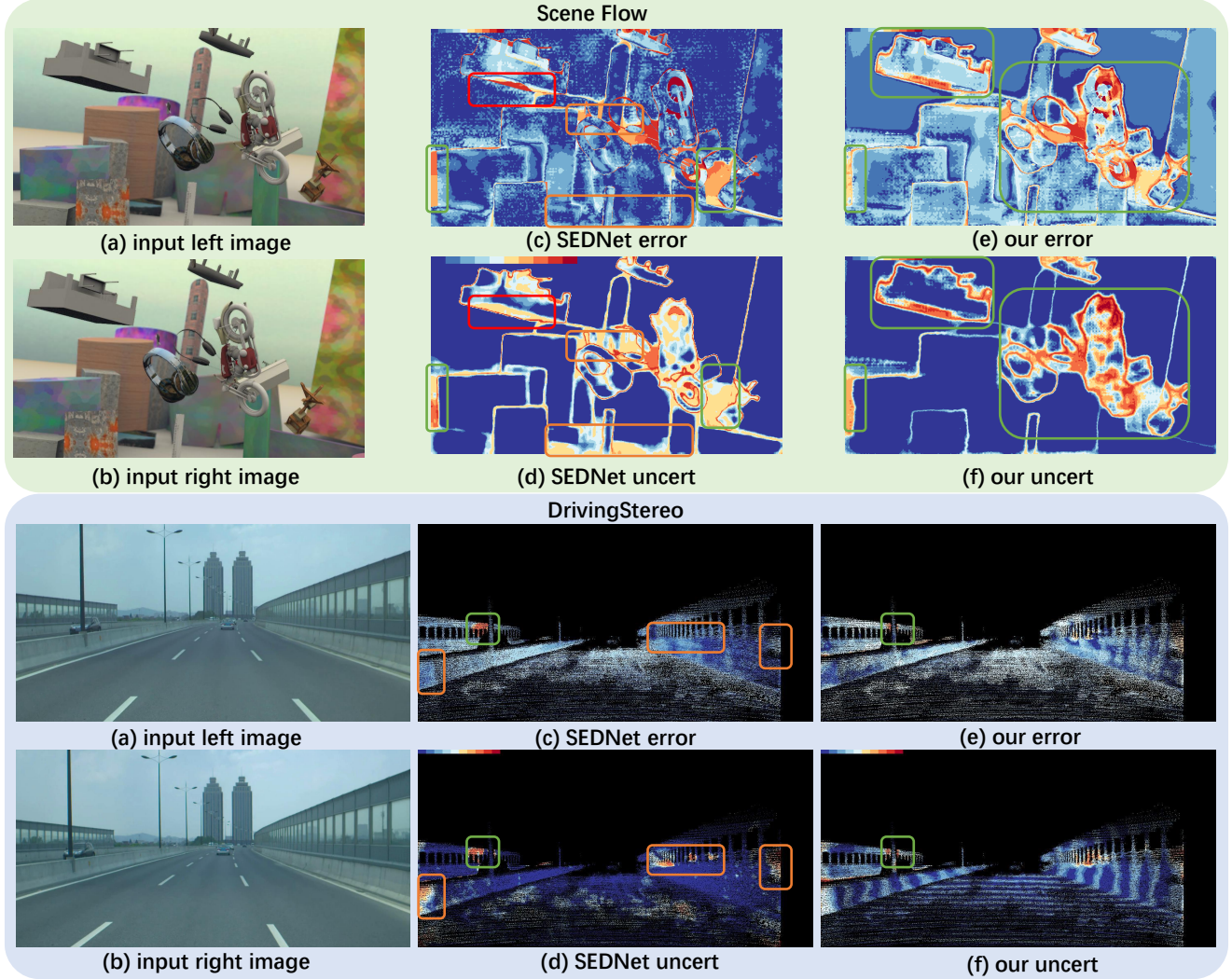


Figure 4. Experimental results of Scene Flow [39] and DrivingStereo [53]. **Red** box: Large error, small uncertainty—model fails to predict large errors. **Orange** box: Small error, large uncertainty—model is overly cautious. **Green** box: uncertainty aligns well with error.

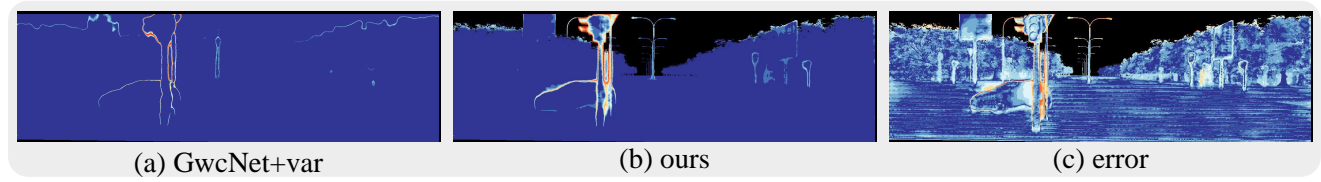


Figure 5. (a) GwcNet [21] variance as uncertainty. (b) Our uncertainty. (c) Errormap.

## 5. Discussion

### 5.1. Ordinal Regression

Fig. 5 demonstrates the proposed trained with smooth-l1 loss and ordinal regression loss (OR loss). Uncertainty estimation of model trained with OR loss aligns better with

error distribution. It provides more detailed information compared with model trained with smooth-l1 loss. OR loss enables the model to better learn the distribution of disparity, while smooth-l1 loss only provides a prediction value in training.

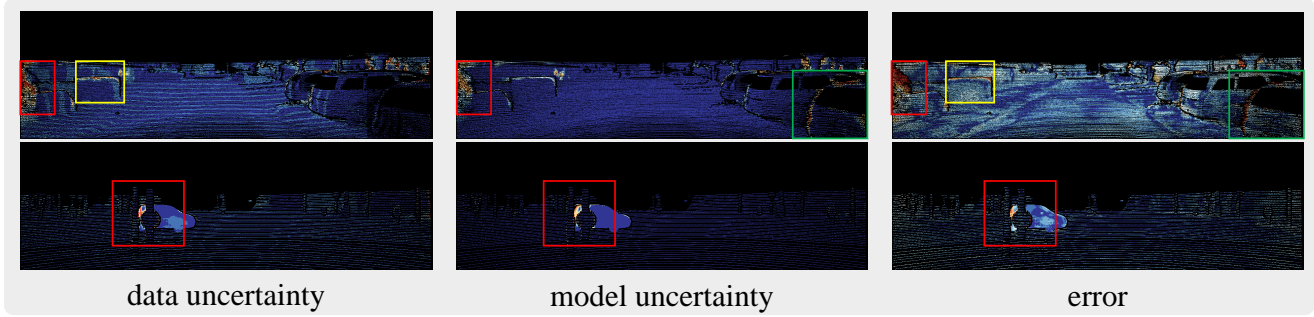


Figure 6. Model and data uncertainty both explains errors in prediction. Areas where data uncertainty matters most are marked with yellow boxes, while areas where model uncertainty explains error are marked with green boxes. Red box indicates that both uncertainty matters.

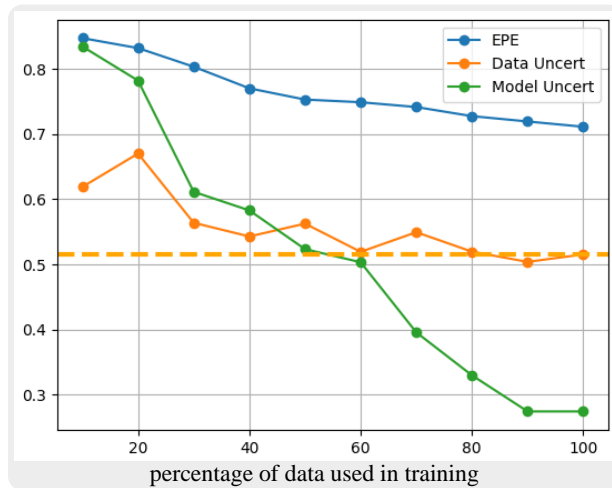


Figure 7. Different proportions of KITTI 2015 [20] training set is used in training, with model pretrained on Virtual KITTI [18]. We report EPE and mean of data and model uncertainty. EPE and model uncertainty decreases are more training data is used. Our estimation of data uncertainty is consistent and reliable when more than 30% of training set is used.

## 5.2. Model Uncertainty Matters

We use a subset of the dataset for training to assess the model’s ability to predict both data and model uncertainty. This training approach has two effects:

- Data and model uncertainty are of the same order of magnitude numerically.
- We can observe that in certain parts of the images, primarily data uncertainty is significant, while in other parts, model uncertainty is predominant. There are also regions where both uncertainties are large. The complementary nature of data and model uncertainty explains the source of errors. Please refer to Fig. 6.

## 5.3. Training Data

The magnitude of model uncertainty reflects the adequacy of model training. Increasing the training data can reduce model uncertainty, even down to 0. We propose that, to simulate the scenario of insufficient model training in reality, training with a portion of the dataset slightly reduces model performance and increases model uncertainty. The magnitudes of EPE, data uncertainty, and model uncertainty follow the trend outlined in Fig. 7. Models here are pretrained on 2000 images from Virtual KITTI [20] and trained on KITTI dataset to demonstrate the trend.

**Application of Uncertainty.** Pixels with large data uncertainty tend to have more random corresponding labels  $Y$  for the same feature  $X$  ( $Y$  has large variance on condition of  $X$ ). The ground truth for these pixels is noisy and can mislead the model. Therefore, we detect data uncertainty and use it to filter out pixels with high data uncertainty. The filtered dataset can improve stereo matching accuracy. In training, our OR model predicts data uncertainty simultaneously with disparity, and we use the predicted uncertainty to mask out high uncertainty data. We call it: training on small uncertainty data (TSUD) [38, 48]. TSUD can also be applied to transfer learning [32, 46] and semi-supervised learning [43, 51, 55]. Since our uncertainty quantification comes directly from the estimated PMF, TSUD does not introduce any extra time or computational costs.

## 6. Conclusion

In this paper, we proposed a novel method for uncertainty quantification in stereo matching, decoupling data and model uncertainty. Our approach utilizes ordinal regression for disparity estimation and kernel regression for model uncertainty estimation. Experimental results on various datasets demonstrated the effectiveness of our method in accurately estimating depth and uncertainty. Additionally, we introduced a training approach to simulate real-world scenarios with pronounced model uncertainty, adding practical significance to our work.

## 7. More Discussions

### 7.1. Kernel Regression

The Deep Ensemble (bootstrapping) [24, 34] require repeated training of the model to estimate model uncertainty, thus demanding significant time and computational resources. According to [16], Monte-Carlo Dropout [7, 12, 19] changes the original Bayesian model and its performance would be worse than Deep Ensemble. We compare the time and model uncertainty estimation performance of KR with Wild Bootstrap (WBS), Multiplier Bootstrap (MBS), and Monte-Carlo Dropout (MCD). Results are reported in Table 2.

Table 2. Wild Boostrap [52], Multiplier Bootstrap [8], Monte-Carlo Dropout [19] and Kernel Regression are compared on Scene Flow dataset [39]. Data uncertainty is estimated with OR. 2000 images are used in training. Our OR+KR fashion is a little bit worse in model uncertainty estimation compared to bootstrapping, but is significantly faster.

Method	WBS [52]	MBS [8]	MCD [19]	KR
AUSE	10.97	<b>10.93</b>	13.66	11.84
Time	12 hrs	12 hrs	4 min	<b>1 min</b>

### 7.2. Limitations

We employ ordinal regression for stereo matching and uncertainty estimation. Due to the ordinal regression’s focus on distribution rather than directly on the disparity values, the effectiveness of the disparity estimation is slightly inferior compared to mainstream methods supervised with smooth L1 loss on some datasets, but the generalization and uncertainty estimation performance is much better.

### 7.3. Broader Impacts

It is important to acknowledge that our paper does not explicitly discuss broader impacts in the proposed method, such as fairness or bias. Uncertainty itself can be utilized in real-world tasks, such as assisting autonomous vehicles in deciding whether to observe the surrounding environment more cautiously. Further research into how our algorithm may interact with other aspects of depth estimation and uncertainty estimation is encouraged.

## 8. More Qualitative Results

We show more image results of error and uncertainty pairs in Fig. 8, 9, 10, 11, 12, 13, 15 and 14.

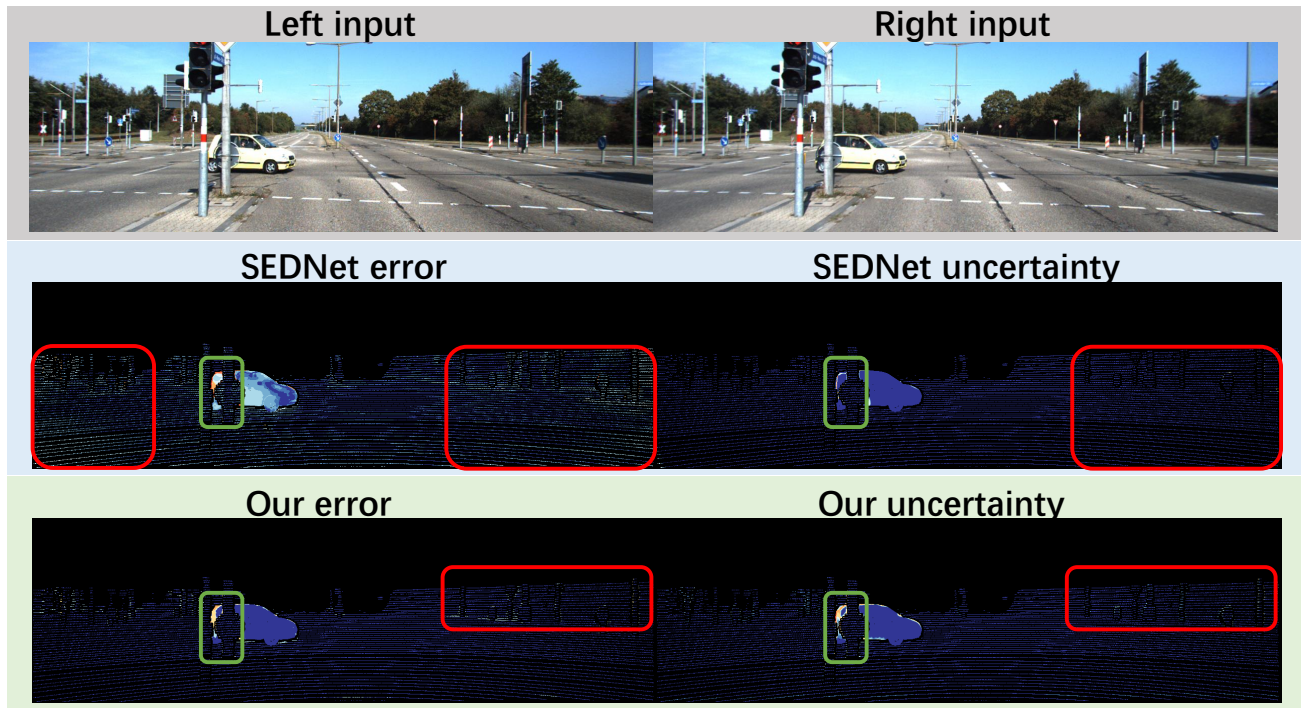


Figure 8. Experimental results on KITTI [20]. **Red box:** Large error, small uncertainty. **Green box:** uncertainty aligns well with error.

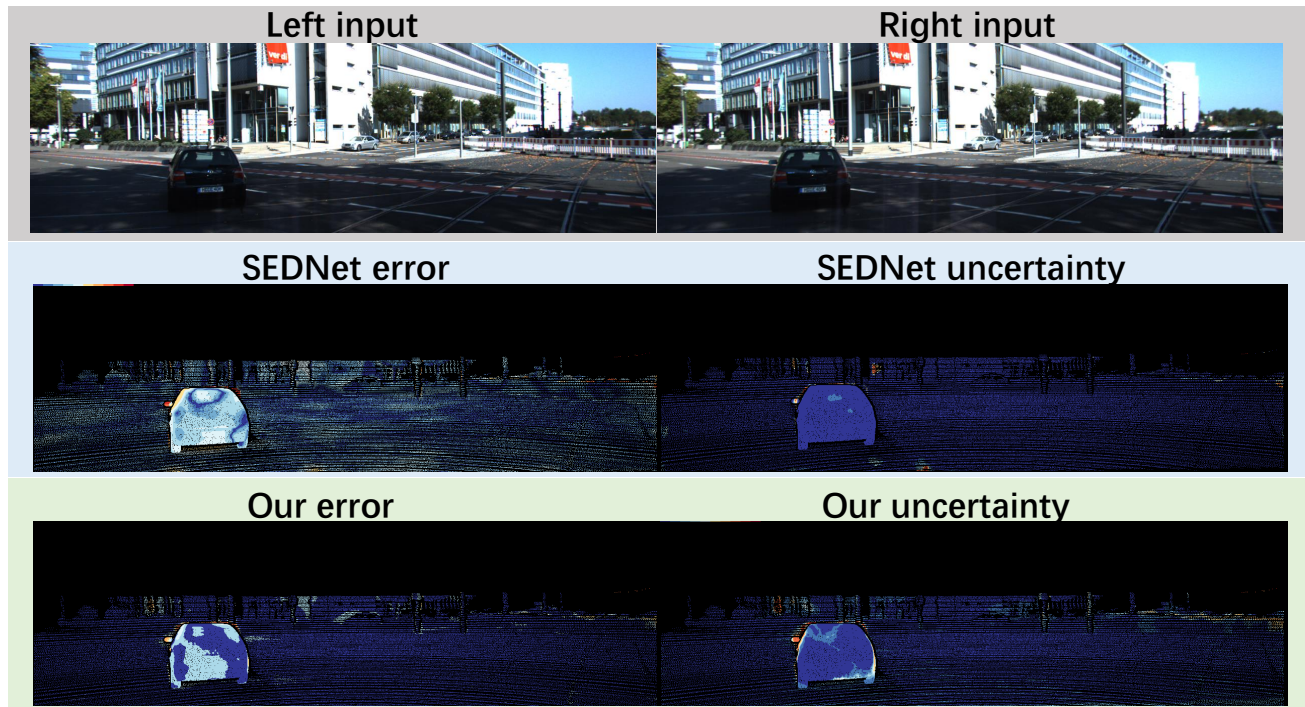


Figure 9. Experimental results on KITTI [20].

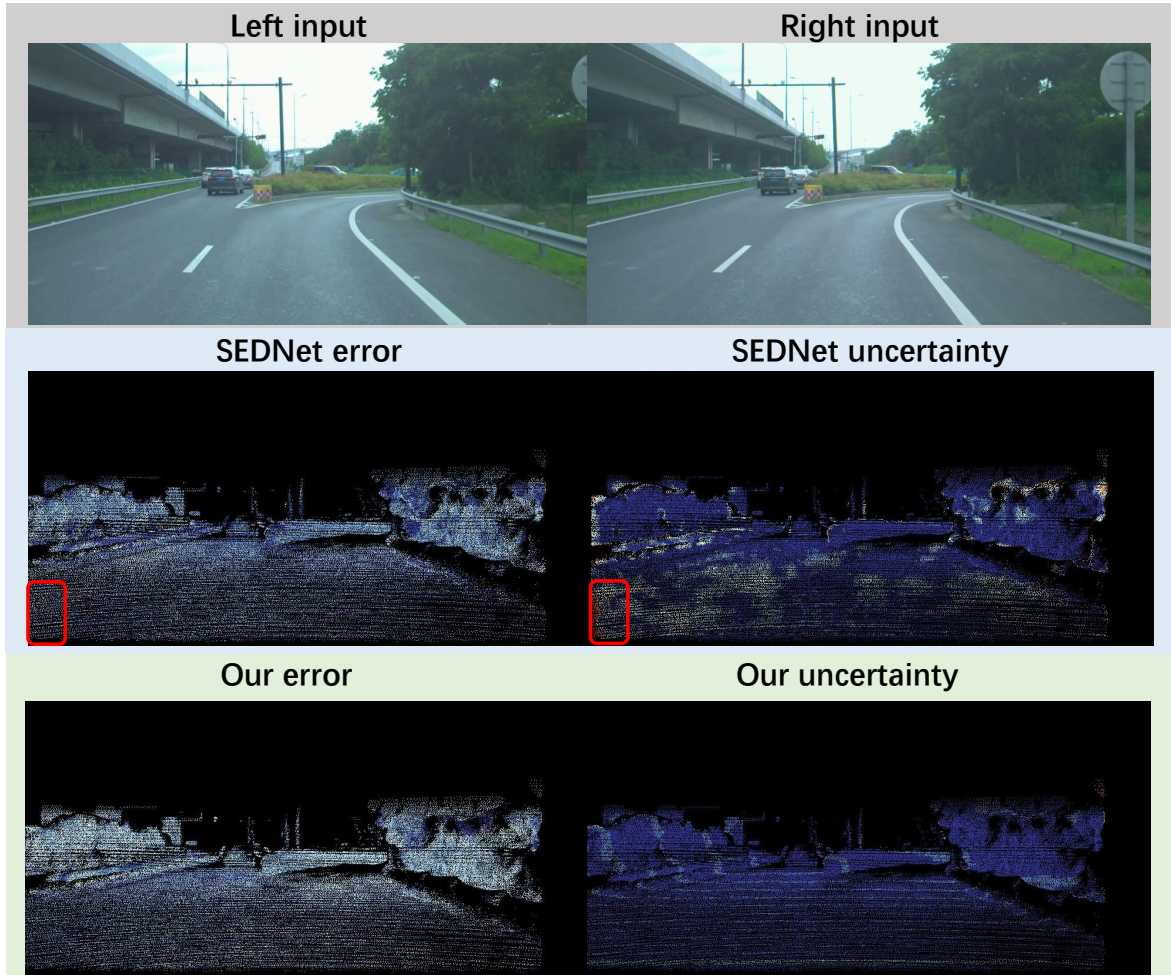


Figure 10. Experimental results on DrivingStereo [53]. **Red** box: Large error, small uncertainty.

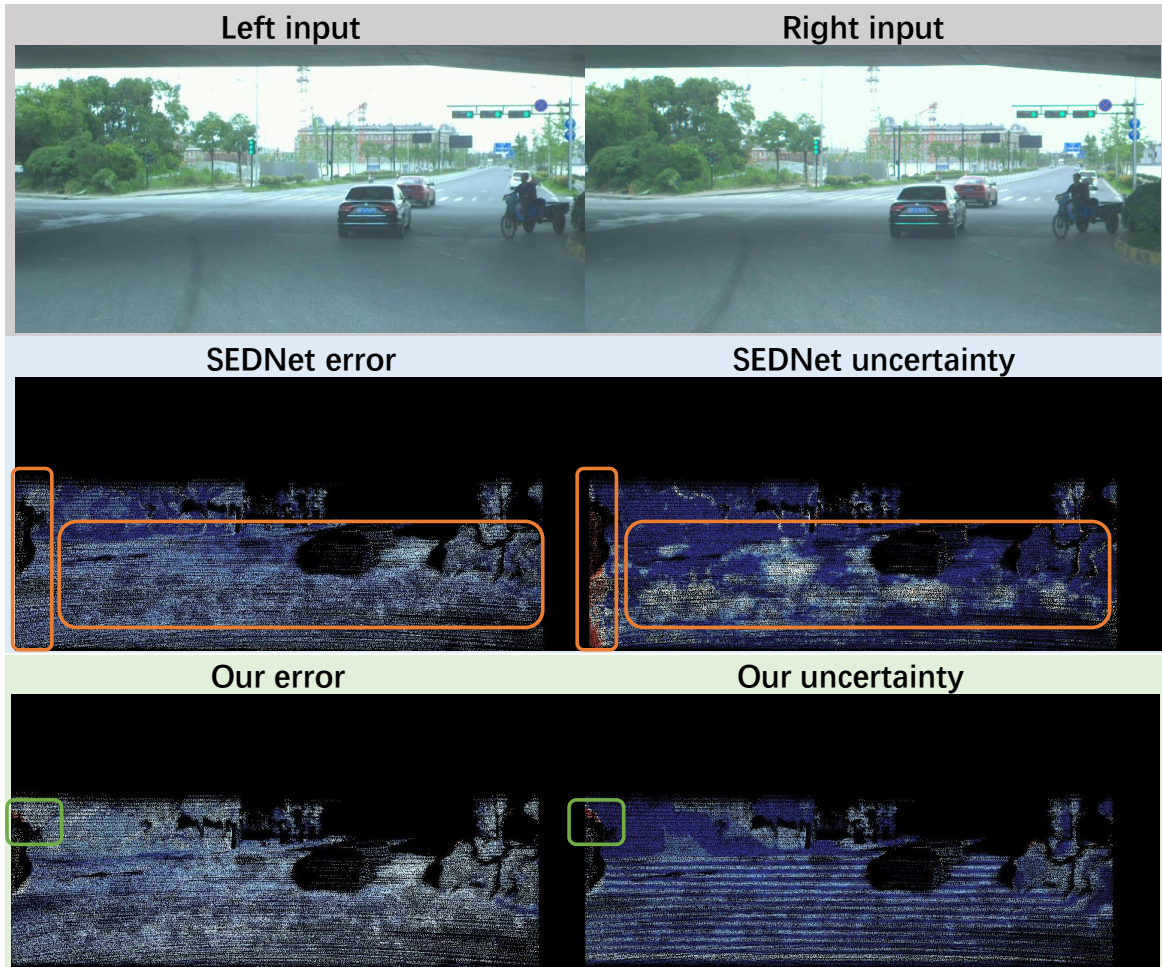


Figure 11. Experimental results on DrivingStereo [53]. **Orange** box: Small error, large uncertain. **Green** box: uncertainty aligns well with error.

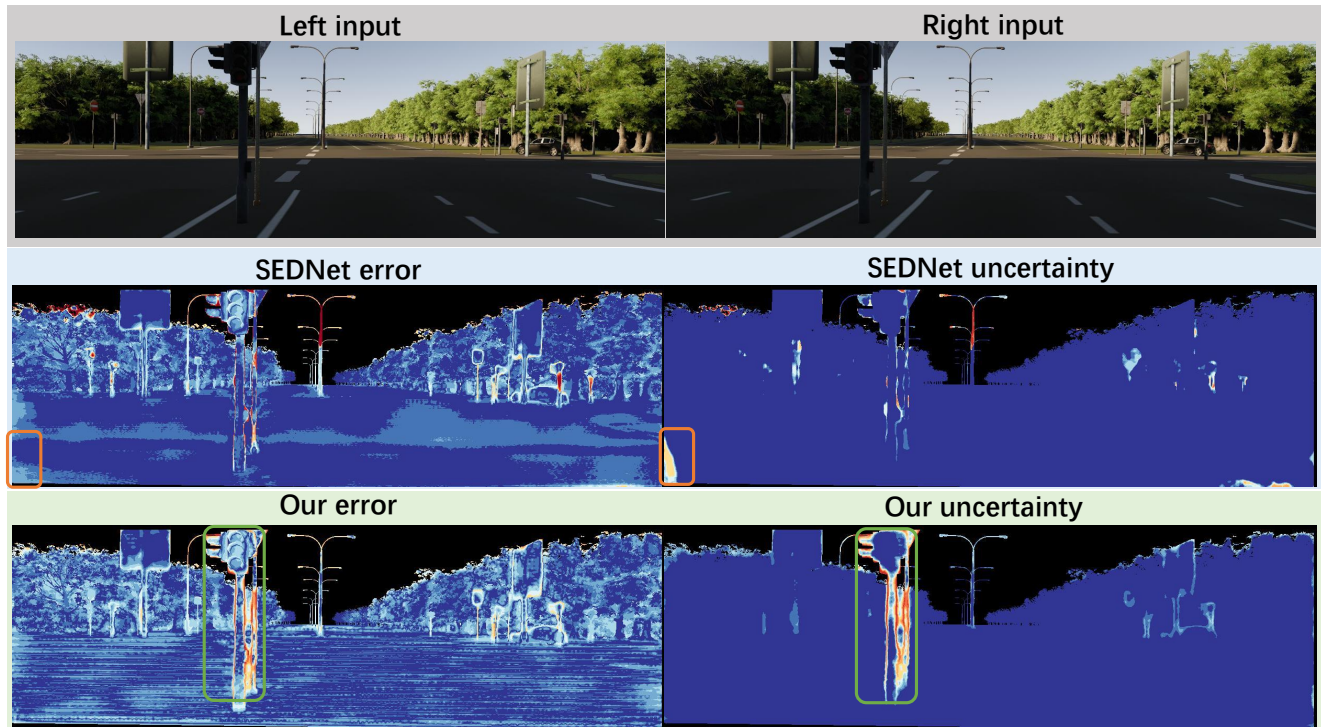


Figure 12. Experimental results on Virtual KITTI 2 [18]. **Orange** box: Small error, large uncertainty. **Green** box: uncertainty aligns well with error.

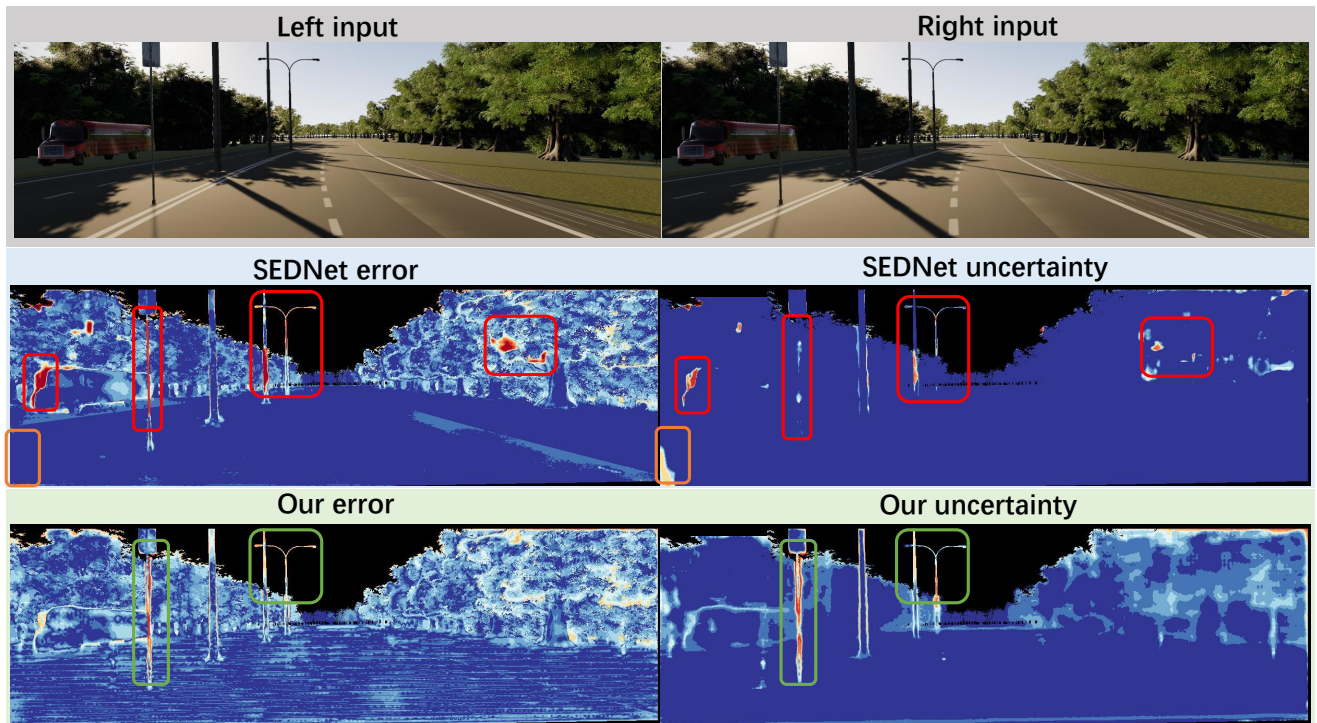


Figure 13. Experimental results on Virtual KITTI 2 [18]. **Red** box: Large error, small uncertainty. **Orange** box: Small error, large uncertainty. **Green** box: uncertainty aligns well with error.

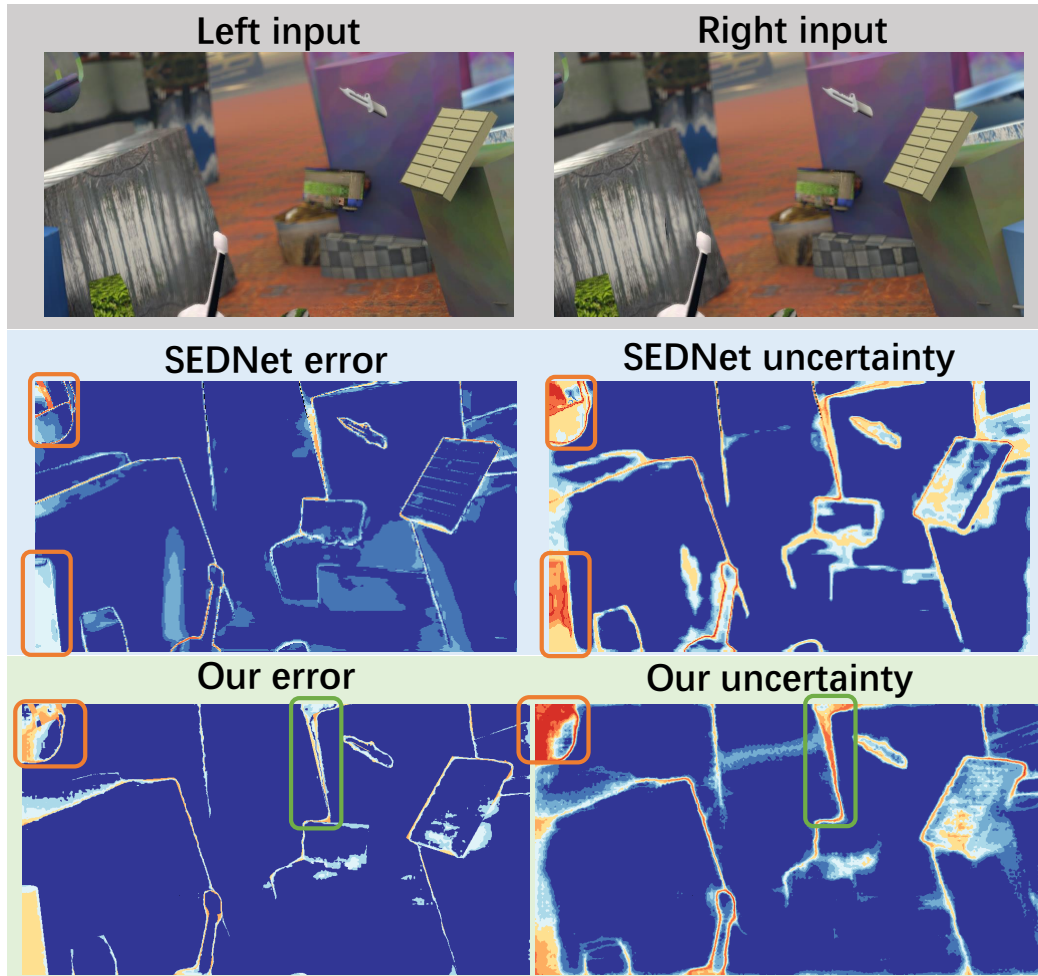


Figure 14. Experimental results on Scene Flow [39]. **Orange** box: Small error, large uncertain. **Green** box: uncertainty aligns well with error.

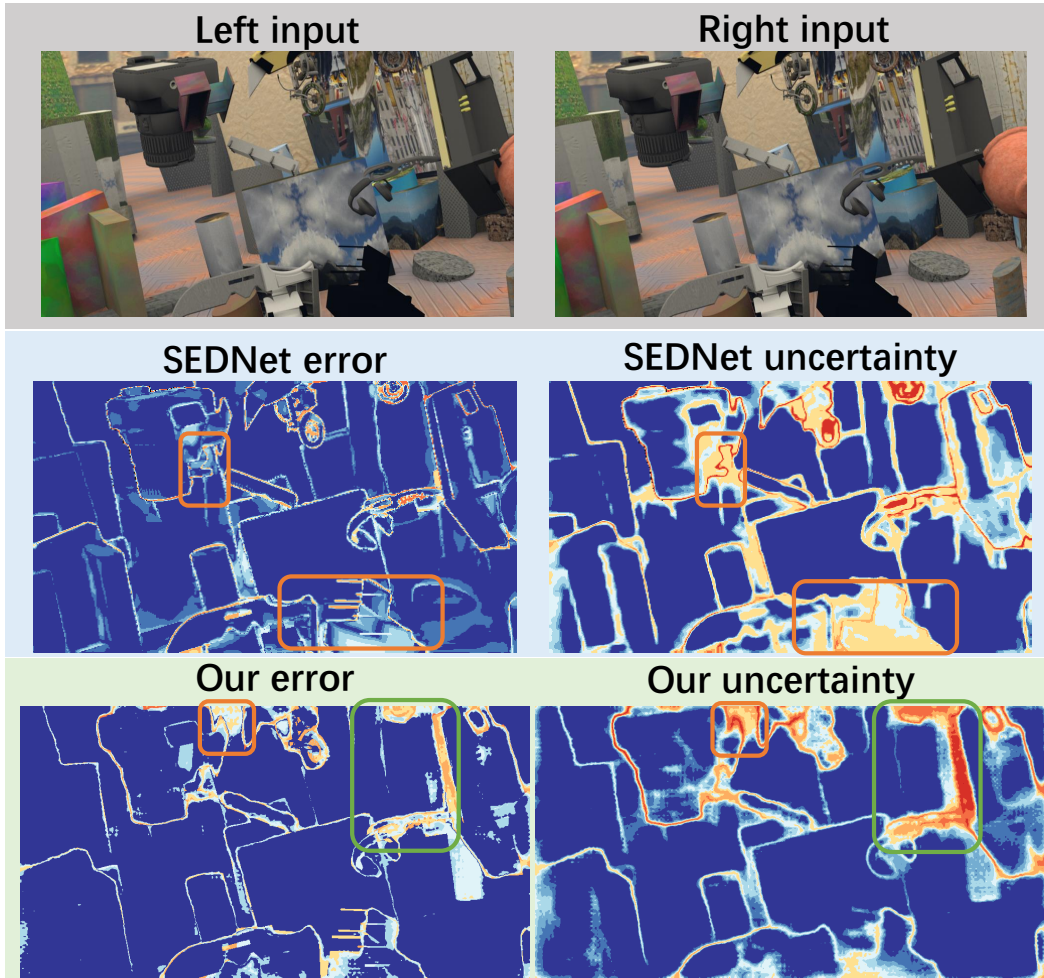


Figure 15. Experimental results on Scene Flow [39]. **Orange** box: Small error, large uncertain. **Green** box: uncertainty aligns well with error.

## References

[1] van Amersfoort, J.R., Smith, L., Teh, Y.W., Gal, Y.: Uncertainty estimation using a single deep deterministic neural network. In: International Conference on Machine Learning (2020), <https://api.semanticscholar.org/CorpusID:263889552> 2

[2] Amini, A., Schwarting, W., Soleimany, A.P., Rus, D.: Deep evidential regression. ArXiv **abs/1910.02600** (2019), <https://api.semanticscholar.org/CorpusID:203836227> 2

[3] Batsos, K., Cai, C., Mordohai, P.: Cbmv: A coalesced bidirectional matching volume for disparity estimation. 2018 IEEE/CVF Conference on Computer Vision and Pattern Recognition pp. 2060–2069 (2018), <https://api.semanticscholar.org/CorpusID:4606944> 2

[4] Blundell, C., Cornebise, J., Kavukcuoglu, K., Wierstra, D.: Weight uncertainty in neural network. In: International Conference on Machine Learning (2015), <https://api.semanticscholar.org/CorpusID:39895556> 2

[5] Chang, J.R., Chen, Y.: Pyramid stereo matching network. 2018 IEEE/CVF Conference on Computer Vision and Pattern Recognition pp. 5410–5418 (2018), <https://api.semanticscholar.org/CorpusID:4252896> 2

[6] Chen, L., Wang, W., Mordohai, P.: Learning the distribution of errors in stereo matching for joint disparity and uncertainty estimation. 2023 IEEE/CVF Conference on Computer Vision and Pattern Recognition (CVPR) pp. 17235–17244 (2023), <https://api.semanticscholar.org/CorpusID:257913707> 2, 5, 6

[7] Chen, T., Fox, E.B., Guestrin, C.: Stochastic gradient hamiltonian monte carlo. In: International Conference on Machine Learning (2014), <https://api.semanticscholar.org/CorpusID:3228832> 2, 9

[8] Chen, X., Zhou, W.X.: Robust inference via multiplier bootstrap. The Annals of Statistics (2019), <https://api.semanticscholar.org/CorpusID:53060424> 5, 9

[9] Cheng, S., Xu, Z., Zhu, S., Li, Z., Li, E.L., Ramamoorthi, R., Su, H.: Deep stereo using adaptive thin volume representation with uncertainty awareness. 2020 IEEE/CVF Conference on Computer Vision and Pattern Recognition (CVPR) pp. 2521–2531 (2019), <https://api.semanticscholar.org/CorpusID:208310189> 2

[10] Dadaneh, S.Z., Boluki, S., Yin, M., Zhou, M., Qian, X.: Pairwise supervised hashing with bernoulli variational auto-encoder and self-control gradient estimator. ArXiv **abs/2005.10477** (2020), <https://api.semanticscholar.org/CorpusID:218763562> 2

[11] Daxberger, E.A., Hernández-Lobato, J.M.: Bayesian variational autoencoders for unsupervised out-of-distribution detection. ArXiv **abs/1912.05651** (2019), <https://api.semanticscholar.org/CorpusID:209319337> 2

[12] Ding, N., Fang, Y., Babbush, R., Chen, C., Skeel, R.D., Neven, H.: Bayesian sampling using stochastic gradient thermostats. In: Neural Information Processing Systems (2014), <https://api.semanticscholar.org/CorpusID:1813746> 2, 9

[13] Dosovitskiy, A., Fischer, P., Ilg, E., Häusser, P., Hazirbas, C., Golkov, V., van der Smagt, P., Cremers, D., Brox, T.: Flownet: Learning optical flow with convolutional networks. 2015 IEEE International Conference on Computer Vision (ICCV) pp. 2758–2766 (2015), <https://api.semanticscholar.org/CorpusID:12552176> 6

[14] Fan, R., Wang, L., Bocus, M.J., Pitas, I.: Computer stereo vision for autonomous driving. ArXiv **abs/2012.03194** (2020), <https://api.semanticscholar.org/CorpusID:227334507> 1

[15] Farooq, A.R., Smith, M.L., Smith, L.N., Midha, S.: Dynamic photometric stereo for on line quality control of ceramic tiles. Comput. Ind. **56**, 918–934 (2005), <https://api.semanticscholar.org/CorpusID:3528482> 1

[16] Folgoc, L.L., Baltatzis, V., Desai, S.R., Devaraj, A., Ellis, S., Manzanera, O.M., Nair, A., Qiu, H., Schnabel, J.A., Glocker, B.: Is mc dropout bayesian? ArXiv **abs/2110.04286** (2021), <https://api.semanticscholar.org/CorpusID:238531665> 9

[17] Fu, H., Gong, M., Wang, C., Batmanghelich, K., Tao, D.: Deep ordinal regression network for monocular depth estimation. 2018 IEEE/CVF Conference on Computer Vision and Pattern Recognition pp. 2002–2011 (2018), <https://api.semanticscholar.org/CorpusID:46968214> 1, 3, 4

[18] Gaidon, A., Wang, Q., Cabon, Y., Vig, E.: Virtualworlds as proxy for multi-object tracking analysis. 2016 IEEE Conference on Computer Vision and Pattern Recognition (CVPR) pp. 4340–4349 (2016), <https://api.semanticscholar.org/CorpusID:1203247> 2, 5, 6, 8, 13, 14

[19] Gal, Y., Ghahramani, Z.: Dropout as a bayesian approximation: Representing model uncertainty

in deep learning. In: International Conference on Machine Learning (2015), <https://api.semanticscholar.org/CorpusID:1607052,9>

[20] Geiger, A., Lenz, P., Stiller, C., Urtasun, R.: Vision meets robotics: The kitti dataset. The International Journal of Robotics Research **32**, 1231 – 1237 (2013), <https://api.semanticscholar.org/CorpusID:94551112,5,6,8,10>

[21] Guo, X., Yang, K., Yang, W., Wang, X., Li, H.: Group-wise correlation stereo network. 2019 IEEE/CVF Conference on Computer Vision and Pattern Recognition (CVPR) pp. 3268–3277 (2019), <https://api.semanticscholar.org/CorpusID:737290842,5,6,7>

[22] Hornauer, J., Belagiannis, V.: Gradient-based uncertainty for monocular depth estimation. ArXiv **abs/2208.02005** (2022), <https://api.semanticscholar.org/CorpusID:2512803452>

[23] Hu, D., Peng, L., Chu, T., Zhang, X., Mao, Y., Bondell, H.D., Gong, M.: Uncertainty quantification in depth estimation via constrained ordinal regression. In: European Conference on Computer Vision (2022), <https://api.semanticscholar.org/CorpusID:2638799552>

[24] Huang, G., Li, Y., Pleiss, G., Liu, Z., Hopcroft, J.E., Weinberger, K.Q.: Snapshot ensembles: Train 1, get m for free. ArXiv **abs/1704.00109** (2017), <https://api.semanticscholar.org/CorpusID:68200061,2,5,9>

[25] Hüllermeier, E., Waegeman, W.: Aleatoric and epistemic uncertainty in machine learning: an introduction to concepts and methods. Machine Learning **110**, 457 – 506 (2019), <https://api.semanticscholar.org/CorpusID:2164653071>

[26] Ilg, E., Çiçek, Ö., Galessos, S., Klein, A., Makansi, O., Hutter, F., Brox, T.: Uncertainty estimates and multi-hypotheses networks for optical flow. In: European Conference on Computer Vision (2018), <https://api.semanticscholar.org/CorpusID:519212416>

[27] Ilg, E., Çiçek, Ö., Galessos, S., Klein, A., Makansi, O., Hutter, F., Brox, T.: Uncertainty estimates and multi-hypotheses networks for optical flow. In: European Conference on Computer Vision (2018), <https://api.semanticscholar.org/CorpusID:519212416>

[28] Kendall, A., Gal, Y.: What uncertainties do we need in bayesian deep learning for computer vision? ArXiv **abs/1703.04977** (2017), <https://api.semanticscholar.org/CorpusID:711341,2,6>

[29] Kendall, A., Martirosyan, H., Dasgupta, S., Henry, P.: End-to-end learning of geometry and context for deep stereo regression. 2017 IEEE International Conference on Computer Vision (ICCV) pp. 66–75 (2017), <https://api.semanticscholar.org/CorpusID:26588602>

[30] Kotelevskii, N., Artemenkov, A., Fedyanin, K., Noskov, F., Fishkov, A., Shelmanov, A., Vazhentsev, A., Petiushko, A., Panov, M.: Nonparametric uncertainty quantification for single deterministic neural network. In: Neural Information Processing Systems (2022), <https://api.semanticscholar.org/CorpusID:2532240562,3,5>

[31] Kuhl, A.: Comparison of stereo matching algorithms for mobile robots (2004), <https://api.semanticscholar.org/CorpusID:167831381>

[32] Lacoste, A., Oreshkin, B.N., Chung, W., Boquet, T., Rostamzadeh, N., Krueger, D.: Uncertainty in multitask transfer learning. ArXiv **abs/1806.07528** (2018), <https://api.semanticscholar.org/CorpusID:493214688>

[33] Lai, X., Xu, X., Zhang, J., Fang, Y., Huang, Z.: An efficient implementation of a census-based stereo matching and its applications in medical imaging. J. Medical Imaging Health Informatics **9**, 1152–1159 (2019), <https://api.semanticscholar.org/CorpusID:1926457371>

[34] Lakshminarayanan, B., Pritzel, A., Blundell, C.: Simple and scalable predictive uncertainty estimation using deep ensembles. In: Neural Information Processing Systems (2016), <https://api.semanticscholar.org/CorpusID:62946741,2,5,9>

[35] Li, J., Yang, Y., chieh Lee, Y.: Overconfident and unconfident ai hinder human-ai collaboration. ArXiv **abs/2402.07632** (2024), <https://api.semanticscholar.org/CorpusID:2676274161>

[36] Li, R.B., Bondell, H.D., Reich, B.J.: Deep distribution regression. Comput. Stat. Data Anal. **159**, 107203 (2019), <https://api.semanticscholar.org/CorpusID:766602842>

[37] Long, Q., Xie, Q., Mita, S., Ishimaru, K., Shirai, N.: A real-time dense stereo matching method for critical environment sensing in autonomous driving. 17th International IEEE Conference on Intelligent Transportation Systems (ITSC) pp. 853–860 (2014), <https://api.semanticscholar.org/CorpusID:171022381>

[38] Lou, J., Liu, W., Chen, Z., Liu, F., Cheng, J.: Elfnet: Evidential local-global fusion for stereo matching. 2023 IEEE/CVF International Conference on Computer Vision (ICCV) pp. 17738–17747 (2023), <https://api.semanticscholar.org/CorpusID:260378744> 1, 2, 8

[39] Mayer, N., Ilg, E., Häusser, P., Fischer, P., Cremers, D., Dosovitskiy, A., Brox, T.: A large dataset to train convolutional networks for disparity, optical flow, and scene flow estimation. 2016 IEEE Conference on Computer Vision and Pattern Recognition (CVPR) pp. 4040–4048 (2016), <https://api.semanticscholar.org/CorpusID:206594275> 2, 5, 6, 7, 9, 15, 16

[40] Mitchell, M.: Why ai is harder than we think. Proceedings of the Genetic and Evolutionary Computation Conference (2021), <https://api.semanticscholar.org/CorpusID:233407771> 1

[41] Mukhoti, J., Kirsch, A., van Amersfoort, J.R., Torr, P.H.S., Gal, Y.: Deterministic neural networks with appropriate inductive biases capture epistemic and aleatoric uncertainty. ArXiv **abs/2102.11582** (2021), <https://api.semanticscholar.org/CorpusID:232014155> 2

[42] Murray, D.R., Little, J.: Using real-time stereo vision for mobile robot navigation. Autonomous Robots **8**, 161–171 (2000), <https://api.semanticscholar.org/CorpusID:1844195> 1

[43] Rizve, M.N., Duarte, K., Rawat, Y.S., Shah, M.: In defense of pseudo-labeling: An uncertainty-aware pseudo-label selection framework for semi-supervised learning. ArXiv **abs/2101.06329** (2021), <https://api.semanticscholar.org/CorpusID:231632854> 8

[44] Schönberger, J.L., Sinha, S.N., Pollefeys, M.: Learning to fuse proposals from multiple scanline optimizations in semi-global matching. In: European Conference on Computer Vision (2018), <https://api.semanticscholar.org/CorpusID:52960429> 2

[45] Seki, A., Pollefeys, M.: Sgm-nets: Semi-global matching with neural networks. 2017 IEEE Conference on Computer Vision and Pattern Recognition (CVPR) pp. 6640–6649 (2017), <https://api.semanticscholar.org/CorpusID:32514247> 2

[46] Shamsi, A., Asgharnezhad, H., Jokandan, S.S., Khosravi, A., Kebria, P.M., Nahavandi, D., Nahavandi, S., Srinivasan, D.: An uncertainty-aware transfer learning-based framework for covid-19 diagnosis. IEEE Transactions on Neural Networks and Learning Systems **32**, 1408–1417 (2020), <https://api.semanticscholar.org/CorpusID:220845561> 8

[47] Shen, Z., Dai, Y., Song, X., Rao, Z., Zhou, D., Zhang, L.: Pcw-net: Pyramid combination and warping cost volume for stereo matching. In: European Conference on Computer Vision (2020), <https://api.semanticscholar.org/CorpusID:253523827> 2

[48] Shen, Z., Song, X., Dai, Y., Zhou, D., Rao, Z., Zhang, L.: Digging into uncertainty-based pseudo-label for robust stereo matching. IEEE Transactions on Pattern Analysis and Machine Intelligence **45**, 14301–14320 (2023), <https://api.semanticscholar.org/CorpusID:260334415> 1, 2, 8

[49] Tsybakov, A.: Introduction to nonparametric estimation. In: Springer Series in Statistics (2008), <https://api.semanticscholar.org/CorpusID:42933599> 4, 5

[50] Wang, X.Z., Nie, Y., Lu, S.P., Zhang, J.: Deep convolutional network for stereo depth mapping in binocular endoscopy. IEEE Access **8**, 73241–73249 (2020), <https://api.semanticscholar.org/CorpusID:218473019> 1

[51] Wang, Y., Zhang, Y., Tian, J., Zhong, C., Shi, Z., Zhang, Y., He, Z.: Double-uncertainty weighted method for semi-supervised learning. In: International Conference on Medical Image Computing and Computer-Assisted Intervention (2020), <https://api.semanticscholar.org/CorpusID:222136511> 8

[52] Wu, C.: Jackknife, bootstrap and other resampling methods in regression analysis. Annals of Statistics **14**, 1261–1295 (1986), <https://api.semanticscholar.org/CorpusID:122946315> 5, 6, 9

[53] Yang, G., Song, X., Huang, C., Deng, Z., Shi, J., Zhou, B.: Drivingstereo: A large-scale dataset for stereo matching in autonomous driving scenarios. 2019 IEEE/CVF Conference on Computer Vision and Pattern Recognition (CVPR) pp. 899–908 (2019), <https://api.semanticscholar.org/CorpusID:195446417> 2, 5, 6, 7, 11, 12

[54] Zbontar, J., LeCun, Y.: Computing the stereo matching cost with a convolutional neural network. 2015 IEEE Conference on Computer Vision and Pattern Recognition (CVPR) pp. 1592–1599 (2015), <https://api.semanticscholar.org/CorpusID:13501868> 2

[55] Zhao, X., Chen, F., Hu, S., Cho, J.H.: Uncertainty aware semi-supervised learning on graph data. ArXiv **abs/2010.12783** (2020), <https://api.semanticscholar.org/CorpusID:2010.12783>

//api.semanticscholar.org/CorpusID:  
225067533 8